

High Harmonic Inverse Free Electron Laser Interaction at 800 nm

Christopher M.S. Sears, Eric Colby, Benjamin Cowan, Robert H. Siemann,
James E. Spencer
Stanford Linear Accelerator Center, Menlo Park, CA 94025

Robert L. Byer, Tomas Plettner
Stanford University, Stanford, CA 94305

March 4th, 2005

We demonstrate for the first time an inverse free electron laser (IFEL) operating at 800 nm and observe multiple resonances of the IFEL interaction. The IFEL is tested at half its fundamental resonance electron energy and scanned through multiple harmonics by adjusting the undulator field strength. We obtain a peak modulation of ~50 keV FWHM and observe the 4th through 6th harmonics of the IFEL resonance.

PAC No: 41.75.Jv, 41.60.Cr

Laser driven accelerators require electron bunches less than the laser wavelength. Current RF injectors for linear accelerators have produced electron bunches as short as a few hundred femtoseconds from photocathode guns [1]. This is still much longer than the few femtosecond periods of lasers for acceleration research [2-6]. To obtain net acceleration and increase capture efficiency, previous experiments used an IFEL plus a magnetic chicane to microbunch the beam ahead of the accelerator [4,5]. These experiments both operated at 10.6 μm and used the fundamental of the IFEL interaction to modulate the electron beam. In this letter, we demonstrate an IFEL at 800 nm and explore the higher harmonics of the interaction.

In theory any acceleration scheme can serve as a microbuncher along with a magnetic chicane used to turn the energy modulation into a longitudinal density modulation. However, the IFEL has many advantages over other modulation methods. Most schemes require apertures on the order of the wavelength, in this case 800 nm. The IFEL, however, has a largely free space interaction with the interaction taking place across the full transverse size of the Gaussian laser beam. To obtain relatively flat phase fronts for the electron microbunching, this spot size is kept fairly large, many 100's of wavelengths. Additionally, the undulator itself has dimensions that are γ^2 larger than the laser wavelength (a few centimeters for this undulator). This makes fabrication far simpler, and simplifies alignment of the electron and laser beams into the IFEL.

The resonance condition for the IFEL interaction is the same as the forward case and given by equation 1 where a_w is the normalized magnetic field of the undulator, λ_w the undulator period, λ_L the laser wavelength, and n the harmonic number [7]. In the case

$$n = \frac{\lambda_w}{2\lambda_L\gamma^2} (1 + a_w^2) \quad (1)$$

Submitted to Physical Review Letters

of a simple sinusoidal undulator field and a plane wave laser the electron undergoes a figure eight motion in the beam frame of reference. Due to the symmetry of the motion the electron couples to frequencies at odd harmonics of the oscillation. However, when the electron has an additional net transverse motion and the full Gaussian laser beam is considered the symmetry breaks and the beam can couple to even harmonics of the motion as well [8]. This is the case for the current experiment where the electrons have an additional transverse motion and both beams are undergoing tight focusing inside the undulator. In this experiment the electron beam energy is half that of the original designed energy, giving a starting harmonic number of $n=4$. Other harmonics are reached by increasing a_w .

Obtaining analytical results for the amplitude of the interaction at each resonance is more difficult. A solution for a single particle interacting with a plane wave can be found relatively simply, but the geometry of this experiment involves Gaussian beams tightly focused, angular intercepts and a short undulator in which the non-periodic end fields cannot be ignored. For this reason, the experiment will instead be compared to simulations that use a simple particle tracker code to propagate a large number of electrons through the undulator in the presence of a Gaussian laser beam. The code integrates the Lorentz equations using the Euler method. A field map of the undulator is loaded from the magnetostatic solver code Radia [9]. Last, the analytic form for a gaussian laser beam is included with the static field.

Parameter	Value
E-beam energy	30 MeV
E-beam initial energy spread (1s)	30 keV (typ.)
E-beam charge	2 pC
E-beam pulselength (1s)	1 ps
E-beam normalized emittance	2π -mm-mrad
E-beam focused vertical width (FWHM)	40 μm
E-beam focused horizontal width (FWHM)	210 μm
Laser pulselength (FWHM)	2 ps
Laser wavelength	800 nm
Laser energy	0.5 mJ
Laser focused spotsize (FWHM)	110 μm

Table 1: IFEL experimental parameters and parameters used in simulation.

Table one summarizes the parameters for the IFEL experiment. The laser is synchronized to the accelerator with an additional phase shifter to allow scanning the laser past the e-beam in time. Both beams come to a focus in the middle of the undulator. This increases the peak field of the laser necessary to obtain an appreciable interaction while maintaining good overlap. The beams are aligned using two phosphor screens located at either end of the undulator.

The laser is introduced into the interaction chamber at an angle of ~ 15 mrad. This eliminates the need for a small chicane to pass the electrons around the last mirror inside the vacuum chamber or a pellicle which would need to be placed far from the focus to avoid laser damage. Also, this experiment was performed in tandem with an inverse transition radiation experiment [10] that requires a laser angle of $\sim 1/\gamma$, or about 15 mrad. To maintain overlap of the electrons and laser inside the undulator along the full electron trajectory, the undulator end fields are de-tuned so that the electrons move with an angle similar to that of the laser (figure 1).

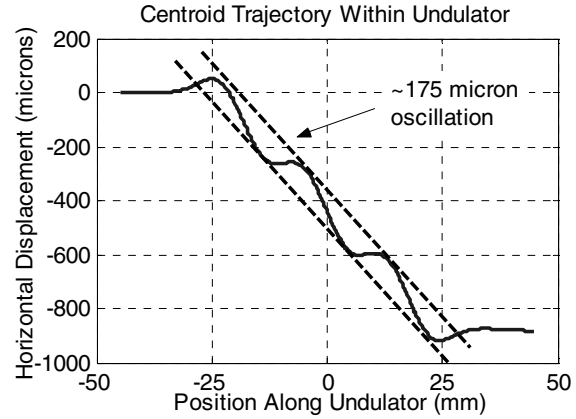


Figure 1: Calculated trajectory of beam from the measured fields of the undulator. The oscillation size increases the horizontal overlap.

The data runs consist of several hundred laser-electron interactions taken at a rate of 10 Hz. Energy spectra are recorded for each electron bunch. For each interaction the offset time between the electron beam and laser is randomly varied over a range of 20-30 picoseconds. In post-analysis, the widths of the energy profiles are calculated to determine the energy spread of the electron beam at each shot. Figure 2 shows an example scatter plot of the electron energy spread after the IFEL with the offset time between the two beams. The cross-correlation signal is clear. The width of the cross-correlation compared to the known laser pulselength gives an e-beam length of ~ 1 ps. A least squares fit (solid curve) gives a mean interaction for ideal temporal overlap. A number of factors cause spreading of the data under the peak of the interaction; including temporal jitter and electron beam pulse length jitter. To factor out this additional spreading, the maximum interaction (dashed curve) is estimated from the strongest interactions of the peak. Comparison between data runs with the same parameters has found that this peak interaction estimate has a factor of two better repeatability between runs compared to the least squares fit amplitude.

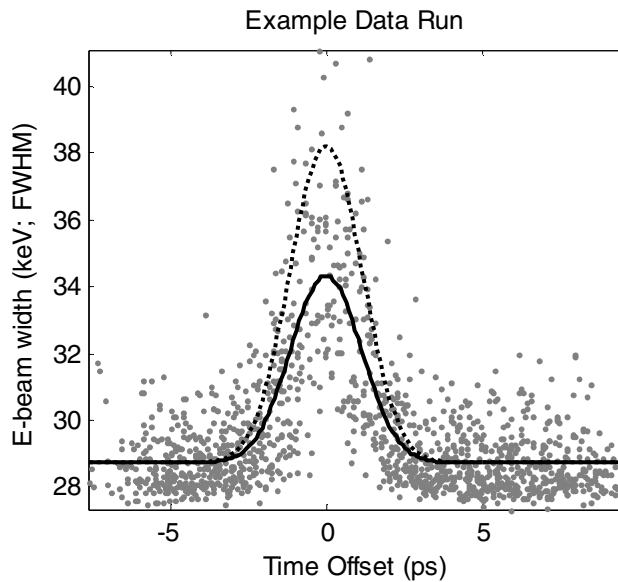


Figure 2. Example data run with 1500 laser on events. Solid curve is least squares fit to all data points, gives mean interaction of 18 keV. Dashed curve is maximum estimate, gives peak interaction of 25 keV. The width of cross-correlation is 2.2 ps rms.

In addition to the time offset scan that occurs with in every run, between runs other experimental parameters are varied to further explore the IFEL interaction. In particular, the transverse overlap is scanned using a mirror located far from the undulator. Also, to observe multiple resonances of the interaction, the gap of the undulator is varied from 4-11 mm.

Results for the horizontal and vertical scans are shown in figure 3. While there are just a few runs for each scan, the data does shown good agreement with simulation. The laser waist is known from a knife edge measurement to be 110 μm FWHM. The vertical overlap, which is a cross-correlation of the two waists, gives an estimate of the vertical electron beam size of 40 μm FWHM. The horizontal overlap is additionally enlarged due to the transverse oscillations of the electrons through the undulator. At 30 MeV this oscillation is $\sim 175 \mu\text{m}$ peak to peak (see figure 1). Comparison to simulation gives a horizontal spot size of 210 μm FWHM. The asymmetric spot shape is confirmed qualitatively from observations of the spot shape noted at the time of the scan.

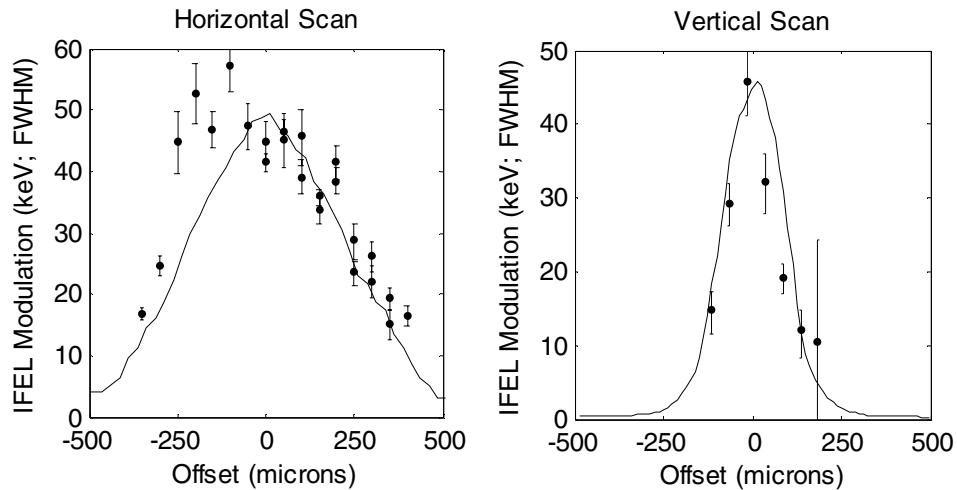


Figure 3: Vertical and horizontal overlap scans. Solid curve is simulation. The horizontal overlap is enlarged due to the horizontal oscillation of the electrons within the undulator.

It is important to note that neither the data nor simulation in figure 3 has been rescaled in energy or offset, the simulation and experiment agree very well for these scans. Within the uncertainty of the runs, we find that 50 keV is the maximum modulation seen for the IFEL interaction. The transverse overlap scans were done with the gap set to 6.3 mm which, as we see in the gap scan data, corresponds to the strongest resonance peak accessible by the experiment.

Compared to the transverse scans the gap scan interaction amplitudes (figure 4) are smaller by $\sim 50\%$. The transverse overlap procedure is accurate to ~ 25 micron, leaving $\sim 10\%$ uncertainty in the interaction amplitude. Also, there are a number of other parameters that can decrease the interaction amplitude including a larger transverse spot size, or longer electron pulse length. Clearly present in the data are two resonances, identified by comparison to simulation as the 5th, and 6th resonances. The 4th order resonance is also clear once it is presented alongside the simulation. Since the change in field strength is less as the gap becomes larger, the 4th order peak is stretched out compared to the other peaks. The simulation also shows additional resonances at still

smaller gap heights; the 7th through 9th, however the data are too noisy to confirm their presence. While one might expect the 4th resonance to have a stronger interaction due to the lower order, there are two effects that change this. First, the coupling methods for even and odd harmonics are different, and under strong diffraction higher harmonics can actually have larger coupling strengths [8]. Second, since the alignment is not changed during the gap scan, as the gap increases the laser-electron overlap diminishes. The increase in gap decreases the magnetic field strength and therefore the electron horizontal motion decreases. This leads to a further roll-off of interaction intensity at large gaps and to a lesser extent as the gap becomes very small (the alignment was done at a gap of 6.3 mm).

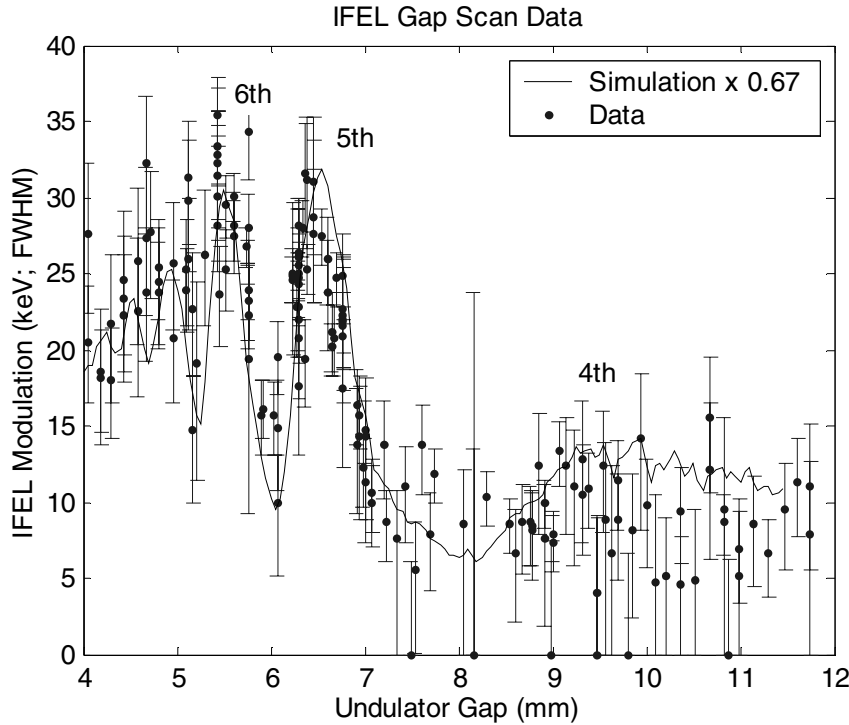


Figure 4: IFEL gap scan data, 164 runs total. Comparison to simulation (solid line) shows very good agreement to the shape and spacing of resonance peaks. The harmonic numbers are given next to each peak. Simulation has been rescaled vertically by 0.67 to better visualize overlap.

Comparison to simulation is complicated by the fact that the overlap diagnostics do not give the absolute position of either beam with respect to the undulator. Therefore, the distance of the electron beam off of the bottom pole tips is not well known. Since the field of an undulator varies as the hyperbolic cosine of the vertical position, the field strength is in turn not well known. However, using the height of the beams as a free parameter in simulation, a best match can be found. Figure 4 gives the best match of simulation to the data where the height of the electrons off of the bottom pole tips is 2.5 mm. The overall amplitude of the simulation is some 50% greater than the raw data, reaching a peak of 50 keV on the 5th harmonic in agreement with the interactions seen during the transverse scans.

With the inclusion of higher harmonics the IFEL can interact over a broad range of parameters. It is worth noting that the 5th and 6th harmonics are comparable in intensity, the IFEL interaction does not necessarily decrease with harmonic number. Both are in fact substantially stronger than the 4th harmonic interaction. With an adjustment of the laser-electron angle the 4th harmonic intensity could also be made stronger. This flexibility extends the utility of undulators or, more simply, aids the experimenter in changing other parameters such as choice of laser wavelength or beam energy.

This experiment has successfully demonstrated the interaction of an 800 nm laser with electrons via the IFEL interaction and observed multiple resonances. There are multiple clearly distinguished peaks in the gap scan data. The relative peak amplitudes and spacing agree quite well with simulation. By adjusting the laser-electron angle back to zero and adding a chicane the IFEL can be used to microbunch beams on the optical scale.

The authors would like to thank Roger Carr of Stanford Synchrotron Radiation Laboratory for simulation and design help for the undulator and contribution of materials. We also thank Todd Smith and the staff of HEPL-SCA for their support and Chris Barnes who did the early simulation work on the IFEL. Last, we acknowledge Pietro Musumeci for useful discussions on higher harmonic theory of FELs. This work supported by Department of Energy contracts DE-AC03-76SF00515 and DE-FG02-03ER41276.

References

1. X. J. Wang *et al.*, Phys. Rev. E **54**, R3121 (1996).
2. W.D. Kimura, *et al.*, Physical Review Letters; 23 Jan. 1995; vol.74, no.4, p.546-9
3. K. Nakajima, *et al.* Physical Review Letters; 29 May 1995; vol.74, no.22, p.4428-31
4. W.D. Kimura, *et al.* Phys. Rev. S.T. Acc. & Beams **4** 101301 (2001)
5. P. Musumeci, *et al.* AIP Conference Proceedings; 2002; no.647, p.278-85
Advanced Accelerator Concepts Tenth Workshop, 22-28 June 2002, Mandalay Beach, CA, USA
6. C.D. Barnes, E.R. Colby, T. Plettner. AIP Conference Proceedings; 2002; no.647, p.294-9
Advanced Accelerator Concepts Tenth Workshop, 22-28 June 2002, Mandalay Beach, CA, USA
7. C.A. Brau. Free Electron Lasers. Boston: Academic Press, c1990
8. W.B. Colson, G. Dattoli, F. Ciocci. Physical Review A. 1985. vol. 31, no. 2 pg 828.
9. O. Chubar, P. Elleaume, J. Chavanne. Journal of Synchrotron Radiation; 1 May 1998; vol.5, pt.3, p.481-4
10. To be published.